Report No. 2
Second Quarterly Report

Covering the Period
1 October 1963 to 31 December 1963

Investigation of MICROWAVE DIELECTRIC-RESONATOR FILTERS

Prepared for:
U. S. ARMY ELECTRONICS RESEARCH AND DEVELOPMENT LABORATORY
FORT MONMOUTH, NEW JERSEY

CONTRACT DA 36-039-AMC-02267(E)
TASK NO. 5544-PM-63-91

By. S. B. Cohn and K. C. Kelly

RANTEC CORPORATION
CALABASAS, CALIFORNIA

Report No. 2

Second Quarterly Report

Covering the Period
1 October 1963 to 31 December 1963

Investigation of MICROWAVE DIELECTRIC-RESONATOR FILTERS

Prepared for:
U. S. ARMY ELECTRONICS RESEARCH AND DEVELOPMENT LABORATORY
FORT MONMOUTH, NEW JERSEY

CONTRACT DA 36-039-AMC-02267(E)
TASK NO. 5544-P.W. 3-91

By. S. B Cohn and K. C. Kelly

Rantec Project No 31625

Approved

Seymour B. Cohn

SEYMOUR B COHN, Technical Director

TABLE OF CONTENTS

SECTION I

PURPOSE

This program is intended to study the feasibility of high-dielectric-constant materials as resonators in microwave filters, and to obtain design information for such filters. Resonator materials shall be selected that have loss tangents capable of yielding unloaded Q values comparable to that of waveguide cavities. The materials shall have dielectric constants of at least 75 in order that substantial size reductions can be achieved compared to the dimensions of waveguide filters having the same electrical performance.

SECTION II

ABSTRACT

The serious effect of air gaps on the measurement of high dielectric-constant values is discussed. Two measurement techniques are described in which air gaps are made to be insignificant sources of error. Both methods utilize resonant modes having zero electric field at dielectric-sample surfaces adjacent to metal walls. In the first method, a cylindrical sample is placed in a close-fitting metal waveguide and resonated in the $TE_{01\delta}$ mode. The air-filled regions of the waveguide on each side of the sample are cut off for the TE_{01} wave so that inappreciable loss of resonant-mode energy occurs. In the second method, a cylindrical dielectric sample is placed at the center of a metallic radial-line pill box. The flat faces of the sample are in contact with the flat walls of the radial line. In this case, also, a circular-electric TE_{01} mode resonance is excited, and the electric field is zero on the sample surfaces. Practical techniques of identifying and measuring the desired resonant frequencies are explained, and exact formulas yielding the dielectric constant are given for both methods. Data obtained by these methods are presented, and the effect of density variation is discussed.

The parameters affecting coupling between dielectric resonators are explained. The basic parameters are magnetic dipole moment, stored energy and resonant frequency of the resonator, and the dimensions of the surrounding enclosure. Formulas are derived for the magnetic dipole moment and stored energy of the dielectric resonator. A generalized formula for coupling coefficient between two magnetic-dipole resonators is derived, and then particularized for the case of dielectric resonators spaced along the center-line of a cut-off rectangular waveguide.

Two pairs of dielectric resonators and three different sizes of waveguides were used to obtain six sets of coupling-coefficient data. The plotted curves can be utilized for design purposes. The measured values are compared to curves computed from the coupling-coefficient formula. The agreement is within ±10 per cent for spacings exceeding about three-quarters of the larger of the two waveguide cross-section dimensions. For smaller spacings, the formula deviates from the measured data due to neglect of higher-mode coupling terms in the derivation. An attempt will be made to add these terms at a later date. In the range of validity of the coupling formula, the accuracy is adequate for ordinary design purposes.

SECTION III

CONFERENCES

On 31 January 1964 a conference was held at the Signal Corps Laboratory in order to discuss progress during the second quarter and plans for the third quarter. Those attending were J. Agrios, J. Charleton, N. Lipetz and E. A. Mariani of the Signal Corps, and S. B. Cohn of Rantec Corp. Results to date indicate utilization of dielectric resonators to be a worthwhile technique in compact microwave filters. It was recognized that temperature-stable materials must be made available before this technique can become fully practical.

SECTION IV

FACTUAL DATA

1. Introduction

The First Quarterly Report[1] discusses the nature of dielectric resonators and describes how such resonators may be used in microwave filters. The introduction to that report should be consulted for background information, and for a discussion of problems to be solved before dielectric resonators can be used in practice.

The accurate measurement of dielectric constant and loss tangent is a basic problem. The materials of interest in this program have dielectric constants in the vicinity of 100, which makes the measurement of dielectric constant highly vulnerable to even very small air gaps. Two methods of measurement are described in detail that are virtually unaffected by air gaps. The dielectric-constant values yielded by these methods are believed to be within a half of one per cent, and certainly within one per cent. Although loss tangent ($\tan\delta$) can be obtained by these methods, more accurate results are achieved by measuring the unloaded Q (Q_u) of a dielectric resonator in a large propagating waveguide (see the First Quarterly Report for details) and then utilizing the approximation $\tan\delta \approx 1/Q_u$. This approximation neglects electric stored energy external to the resonator and losses on surrounding metal walls, but these sources of error are generally small in the cases of interest.

Practical filter design requires data on resonator coupling. Because of the large number of parameters involved, it is not feasible to obtain a quantity of experimental data adequate for all needs. Therefore, it is essential to have a formula for coupling coefficient that is sufficiently accurate and simple to be practical for ordinary design

purposes. An analysis of coupling was carried out during the second quarter, and is treated in this report. The resulting formula meets the dual goals of accuracy and simplicity. However, the neglect of higher-order coupling terms limits the formula to coupling coefficients less than about 0.02. By adding more terms, an extension of the range of validity should be possible, permitting closer spacings and therefore larger coupling coefficients. The analysis in this report is sufficiently general to lay the groundwork for this extension. Also, the formulas for magnetic dipole moment, stored energy, and generalized coupling will prove useful for other computations to be made later.

A series of coupling-coefficient measurements were made in order to provide some initial design data and enable the accuracy of the coupling formula to be ascertained. In the range of validity of the formula, the agreement was within ±10 per cent.

2. Dielectric Constant Measurement

a. Method Chosen for Microwave Measurement of High Dielectric Constants

At dc and low frequencies, the determination of dielectric constant is usually based on measurement of capacitance or capacitive reactance of a parallel-plate capacitor containing the dielectric under test. At microwave frequencies, the dielectric constant is determined through measurement of the effects of the enhanced capacitance produced by the dielectric material. These effects include a change in velocity of propagation in a dielectric-loaded transmission line, a change in the resonant frequency of a dielectric-loaded resonant cavity, and reflections at the boundaries. However, the new capacitance or capacitance per unit length is unpredictably introduced if electric field lines pass through the dielectric to the conducting boundaries by way of irregular or unknown air-gaps.

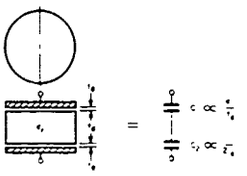

Figure 2-1. Dielectric Capacitor with Air Gaps

Figure 2-1 illustrates the parallel-plate-capacitor case, in which the electric field passes through the dielectric and the air gap. Air gaps of average thickness, t_a, will exist in practice, unless all mating surfaces are perfectly smooth and flat. Alternatively, a conductor may be plated on the dielectric sample as a defense against air gaps. Failing to do either, the effective capacitance of the series combination of dielectric capacitor and air capacitor is proportional to

$$C_{total} \propto \frac{\epsilon_r}{t_d + 2t_a\epsilon_r} \tag{2-1}$$

where ϵ_r is the true value of relative dielectric constant. However, neglect of the air-gap effect might lead to computing an incorrect value ϵ_r' from

$$C_{total} \propto \frac{\epsilon_r'}{t_d + 2t_a} \approx \frac{\epsilon_r'}{t_d} \tag{2-2}$$

Setting Eq. 2-1 equal to Eq. 2-2 and solving for ϵ_r' yields

$$\epsilon_r' = \frac{\epsilon_r}{1 + \frac{2t_a\epsilon_r}{t_d}} \tag{2-3}$$

In the present program we are concerned with samples for which t_d is on the order of 0.1 inch and ϵ_r is on the order of 100. Because of surface roughness, imperfectly parallel surfaces, etc., t_a is expected to

approach 0.0001 inch despite considerable care. Thus the ratio of indicated to true ϵ_r is on the order of 0.833. Re-stated, we find that for the case of interest an indicated dielectric constant 17% lower than actual will result from the presence of difficult-to-avoid air gaps as small as 0.0001 inch. The above described effects also operate in a resonator or transmission line when the normal component of electric field, E_n, is not zero on the dielectric surface.

Two methods by which the above difficulties may be avoided at microwave frequencies are based on resonator configurations operating in modes for which $E_n = 0$ on faces of the dielectric sample adjacent to metallic surfaces. This approach is far more practical and economical than metal plating of surfaces of the sample, or extreme dimensional tolerances on sample and holder. In the first method, a sample in the shape of a right-circular cylinder is resonated in a close-fitting circular waveguide that is below cutoff in its air-filled regions. The second technique is similar except that the transmission line used is a radial waveguide. In both cases, the resonant mode of interest is one in which the E-field is parallel to dielectric surfaces and practically zero in air-gap regions.

b. The Circular Waveguide Dielectrometer

Figure 2-2 illustrates the geometry of the circular waveguide dielectrometer. Note the similarity to the configuration described in Figure 2-4 of the Last Quarterly Report of this series.[1] The hypothetical magnetic-wall waveguide boundary described there is replaced by an electric-wall (metallic) waveguide boundary. Exact solutions for resonance are readily obtained for

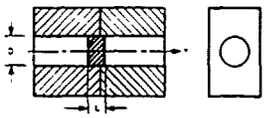

Figure 2-2. The Circular Waveguide Dielectrometer

the present case. Thus, determinations of ε_r are possible after measurement of the resonant frequency of a sample of known dimensions when the resonant mode is such that air gaps are unimportant.

The lowest-order mode resonance for which the normal electric field, E_n, is zero over the surface of the dielectric, as required to make air-gap effects negligible, is the $TE_{01\delta}$ resonance. Assuming negligible losses, the admittances at the surface of the sample in the planes $Z = \pm L/2$ are purely susceptive. Resonance occurs when

$$B_a + B_d = 0 \tag{2-4}$$

The air region is designed to be below cutoff and thus presents a normalized susceptance equal to the characteristic admittance of the air-filled waveguide, as follows.

$$B_a = -\sqrt{\left(\frac{\lambda}{0.820D}\right)^2 - 1} \tag{2-5}$$

Equation 2-5 implies that the cut-off waveguide extends to plus and minus infinity. In practice, insignificant error is incurred when the air-filled waveguide is terminated at a length at which the evanescing wave is attenuated by >30 db. Looking into the dielectric [illegible] normalized susceptance of

$$B_d = \frac{\lambda}{\lambda_g} \tan \frac{\beta L}{2} \tag{2-6}$$

Where, in Eqs. 2-5 and 2-6,

λ = free space wavelength at the resonant frequency

D = diameter of waveguide and of sample

$$\lambda_g = \frac{\lambda}{\sqrt{\epsilon_r - \left(\frac{\lambda}{0.820D}\right)^2}}$$

$$\beta = \frac{2\pi}{\lambda_g}$$

These equations are readily derived from transmission line equations given by Marcuvitz.[2]

Equation 2-4 is a transcendental equation that may be solved for ϵ_r since all other quantities involved may be measured directly. Employment of this technique presents a few practical problems. The principal problem is recognizing the $TE_{01\delta}$ mode amidst the $TE_{11\delta}$, the $TM_{01\delta}$, the $TM_{11\delta}$, etc., resonances that also appear. The solution to this problem points out an additional reason for using the TE_{01} mode. It is the only mode that does not produce longitudinal currents on the conducting walls of the circular waveguide. Thus, when the two bored blocks shown in Figure 2-2 are separated slightly, the $TE_{01\delta}$ resonance is only minutely affected while the other resonances are markedly affected. In practice, this $TE_{01\delta}$ resonance recognition technique operates very effectively after brief practice on the part of the user. Note that the test sample is not centered on the gap. This is done to avoid the standing wave current null that occurs at the center of the sample.

Two pairs of bored blocks were fabricated. Bores of 0.2344 and 0.3438 inch were chosen to handle the variety of dielectric samples on hand. A further objective of using two diameters was to demonstrate that there are no second-order effects that might affect the accuracy as D/L varies. Finally, the use of two values of D aided determination of any frequency dependence of the dielectric constant of a given batch of material.

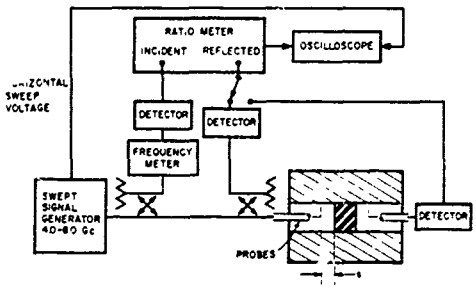

Figure 2-3. Laboratory Instrumentation for Observation of Resonances

Figure 2-3 illustrates the laboratory set-up employed to observe the resonances of samples placed in the circular waveguide dielectrometer. The probes, which couple to the structure, are formed by exposing roughly 3/16-inch of the end of the center conductor of a small diameter rigid coaxial line. The exposed center conductor is bent and the coaxial line inserted so that a section of the probe's length is parallel to a desired electric field line. The choice of transmission versus reflection observation of resonances is a matter of user's preference. The instrumentation shown in Figure 2-3 is suitable for either. So great is the attenuation per unit length in the cut-off waveguide enclosing the probe that the probe is rather close to the sample when resonances are visible on the oscilloscope. When the probe is moved still closer without affecting the resonant frequency, one can be sure that there is no effect of the probe on the resonant frequency of the sample. Since the dielectric constant of the material to be tested is usually known approximately, the process of detecting the TE_{01} mode resonance is aided if the resonant frequency is computed to direct the operator's attention to the correct portion of the frequency sweep.

An initial test with a sample having D = 0.3434 inch and L = 0.1184 inch produced a figure of $\varepsilon_r = 86.9$ for a polycrystalline TiO_2 sample supplied by American Lava Corporation. The diameter of this sample was reduced to 0.3424 inch to illustrate the insensitivity to air-gap size. As expected, the resonant frequency did not change as far as observation with the aid of a high Q cavity frequency meter could

show. The insensitivity to air-gap size, for the case where $E_n = 0$ on the sample's surface, may be visualized by noting that the cut-off wavelength of the dielectric loaded TE_{01} circular waveguide is as follows when t_a/D is small.

$$\lambda_c = 0.820\,(D + 2t_a)\sqrt{\epsilon_r} \qquad (2\text{-}7)$$

Equation 2-7 results from a simple application of perturbation theory. D is the diameter of the sample and t_a is the thickness of an air gap assumed to surround the sample. The error in Eq. 2-7 is proportional to $(t_a/D)^3$, and is very small. Thus, if the diameter of the waveguide surrounding the sample is used for D in Eqs. 2-5 to 2-7, the effect of a small air gap will be negligible.

Four samples (A_1 through A_4 in Table 2-1) from a given batch of relatively pure polycrystalline TiO_2 were ground to nominal diameters of 0.2340 or 0.3434 inch. These samples were selected from a large group supplied by American Lava Corporation. The dielectric constant computed from measured TE_{016} resonant frequencies (5834, 5580, 7585, 5532 Mc for A_1 to A_4, respectively) varied from $\epsilon_r = 78.2$ to $\epsilon_r = 86.9$. These results caused initial surprise since all the samples were claimed to be from the same mix and pressed on the same machine without undue time lapse. A review of the techniques used in determination of ϵ_r reaffirmed the expectation of fractional per cent accuracy. After a careful remeasurement of the dimensions of the samples, each was weighed on an analytical balance. The computed densities showed considerable variation and explained the variation in ϵ_r. Figure 2-4 shows the ϵ_r of the four samples related to the density of each.

With confidence in the usefulness of the circular waveguide dielectrometer justified, a sample from Rantec's more limited

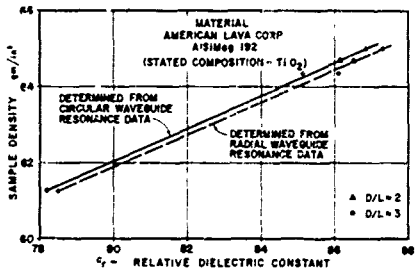

Figure 2-4. Measured Dielectric Constant Values Related to Sample Densities

supply of USAERDL polycrystalline TiO_2 was ground to 0.3434 inch diameter and 0.140 inch length (Sample S_1 in Table 2-1). The dielectric constant was computed from the data to be 97.6 at 72°F and 5024 Mc. There was no indication that the dielectric constant is seriously frequency dependent, but the temperature dependence was evident though not measured.

TABLE 2-1

IDENTIFICATION OF POLYCRYSTALLINE TiO_2 SAMPLES

Sample	Source	D (inch)	L (inch)	Density gm/in^3
A_1	American Lava Corporation	0.3435	0.1180	61.29
A_2	American Lava Corporation	0.3427	0.1183	64.34
A_3	American Lava Corporation	0.2342	0.1162	64.69
A_4	American Lava Corporation	0.3433	0.1185	65.01
S_1	USAERDL	0.3432	0.1400	65.63

The density variation observed with samples from a given batch of material points up the importance of a high level of quality control in every step of the compounding and pressing of polycrystalline samples.

c. Radial Waveguide Dielectrometer

The circular waveguide dielectrometer places a marked constraint on the diameter of the sample to be tested. The radial

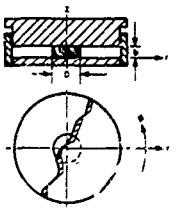

Figure 2-5. The Radial Waveguide Dielectrometer

waveguide dielectrometer does not present this problem and thus offers greater freedom in sample selection. All that is needed is a parallel-plate region whose spacing is set by the length of the right-circular cylindrical sample. Auxiliary structure to keep the plates parallel is useful. In the experiments to be described, the upper plate was the face of a close fitting piston in a cylinder terminated in a surface that formed the bottom plate. (See Figure 2-5.) Again, it is necessary to limit concern to modes for which $E_n = 0$ over the surface of the sample. The TE_{01} mode in radial waveguide satisfies this condition. (The subscript 01 denotes zero variation of the fields from $\phi = 0$ to 2π, and a single maximum in E_ϕ between $z = 0$ and $z = L$. It should be noted that the radial waveguide modes are not generally described as TE or TM. Generally, radial waveguide modes are hybrid with respect to field components in the propagation direction, r.) The usefulness of the unit for determining ε_r is based on observing the frequency of the TE_{01} mode resonance in the dielectric sample under the condition that the TE_{01} mode is below cutoff in the air-filled region of Figure 2-5.

Equation 2-4 still describes the resonance condition, but now[3]

$$B_a = K_a \tag{2-8}$$

and

$$B_d = K_d\left(\frac{J_0(K_a D/2)}{J_1(K_a D/2)}\right) \tag{2-9}$$

where both B_a and B_d are normalized in the same manner. Here

$$K_a = \sqrt{\left(\frac{\pi}{b}\right)^2 - k^2} \tag{2-10}$$

$$K_d = \sqrt{k^2 \epsilon_r - \left(\frac{\pi}{b}\right)^2} \tag{2-11}$$

k = free space phase constant = $2\pi/\lambda$

b = sample height, L

The Bessel functions of the first kind and of order zero and one are indicated by J_0 and J_1 respectively. The admittance indicated by Eq. 2-10 applies to an infinite radius of cut-off waveguide. Practically, the attenuation per unit length is such that negligible error occurs when the line is terminated at a radius of one inch or so.

In operation of the radial waveguide dielectrometer unit, a simple probe is inserted to couple as loosely as will allow adequate resonance indication on the oscilloscope. The sample sizes were such that the field attenuation in the air-filled radial line region outside of the sample is on the order of 200 db/inch for the TE_{01} mode. Probe-to-sample spacings as small as an eighth of an inch were found to give good resonance indication with no shifting of the resonant frequency.

The probe couples to a multiplicity of modes. Many resonances are visible on the oscilloscope. All of the resonances of the several E-type ($E \neq 0$) radial waveguide modes are easily eliminated by noting which resonances move lower in frequency when pressure on the upper plate reduces the minute air gaps due to surface roughness (without measurable change in the plate spacing). The pressure producing the effect is far less than required to mechanically deform the

resolved. In addition to the possibility that measurement errors have different effects on the two methods used, there is the possibility that the temperature of the laboratory was, in fact, quite different during the two sets of measurements. The 72°F temperature reported above for both sets of measurements is based on the laboratory thermostat setting. A recent check shows that a variation of ±4°F was possible. Inhomogenities in the pressed samples or effects of slightly non-parallel faces on the samples also seem to be likely causes. The field distribution in the samples are quite different in the two resonance modes though circular electric field lines are common to both. Whatever the cause of the discrepancy, Sample A_2 is the most serious example. Attention will be focussed on Sample A_2 for the diagnostic work planned.

One important consequence of the dielectrometer results relates to the findings summarized in Figure 2-5 of the First Quarterly Report of this series. With metal boundaries far removed, the calculated and measured resonant frequencies of various samples of USAERDL TiO_2 disagreed by approximately 10 per cent when ϵ_r was assumed to be 100 in the calculations. The disagreement was reduced when the dielectric constant was assumed to be 83.8. The present dielectrometer measurements have established that the ϵ_r of the material in question is not less than 97. Thus, one may conclude that the second-order $TE_{01\delta}$ solution is inadequate for accurate computations of the resonant frequency of dielectric resonators in free space.

3. Analysis of Dipole Moment, Stored Energy, and Coupling

a. Parameters Affecting Coupling

In order to utilize dielectric resonators in a band-pass filter, it is necessary to couple the desired number of resonators to

each other, and to couple the end resonators to terminating transmission lines or waveguides. The bandwidth, pass-band response, and stop-band response depend upon the coupling values and number of resonators, as in the case of any other type of multi-resonator filter. Formulas exist in the literature for computing the required coupling values to achieve the required bandwidth with maximally flat or equal-ripple response shape.[4,5] In this report, a formula is derived relating the coupling coefficient between a pair of resonators to the physical and electrical parameters of the dielectric resonators, their center-to-center spacing, and the dimensions of the surrounding structure.

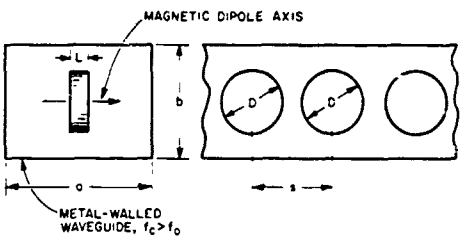

Figure 3-1. Coupled Dielectric Resonators Inside a Rectangular Metal Tube

Figure 3-1 shows the arrangement considered. The resonators are assumed to be cylindrical disks on the center line of a cut-off waveguide. The waveguide serves as a shield, preventing radiation loss and undesired coupling to external fields. The rotational axes of the disks are in the direction of the transverse a dimension of the waveguide. As discussed in the First Quarterly Report, the external field of the fundamental resonant mode resembles that of a magnetic dipole directed along the axis of the disk. Because of this fact, an energized resonator will excite a TE_{10}-mode wave. The amplitude of this wave attenuates with longitudinal distance, since the waveguide is used below its cut-off frequency. The H field of the wave excites the adjacent resonator, resulting in magnetic coupling between the pair of resonators. Because of the exponential decay of the TE_{10} mode, coupling between nonadjacent resonators can usually be neglected.

The coupling geometry of Figure 3-1 appears to be particularly useful. Certain other band-pass configurations that may be of value will be considered in later reports. Another important case is identical to Figure 3-1, but with $\lambda_o < 2a$, or $f_o > f_c$. In this case the TE_{10} mode propagates without attenuation. The result is a band-rejection response rather than band pass. This will also be studied in a later report.

As will be apparent from the analysis, the basic parameters of a resonator influencing its coupling to another resonator are its magnetic dipole moment, stored energy, and resonant frequency. Computation of the magnetic dipole moment and stored energy require a knowledge of the internal and external fields of the resonant mode. These fields are not known exactly, but are approximated by the second-order solution treated in the First Quarterly Report.[1,6] These second-order field functions will be used for the calculations in this report. Fortunately, the resulting coupling-coefficient value appears to be quite insensitive to variations in the assumed field. The resonant frequency may be computed by the second-order formulas,[1] or may be measured. The experimental data in the First Quarterly Report shows measured resonant frequencies to be about ten per cent greater than second-order theoretical frequencies. The measured coupling coefficient values described later in this report agree best with calculated coupling values when measured frequencies are used in the computation.

b. Magnetic Dipole Moment

The magnetic dipole moment $\underline{m}$ is defined in terms of an electric current distribution as follows:[7]

$$\underline{m} = \frac{1}{2} \iiint \underline{R} \times \underline{J} \, dv \qquad (3-1)$$

where $\underset{\sim}{R}$ is the vector distance from an arbitrary fixed reference point, $\underset{\sim}{\imath}$ is the current density, and the integration is performed over a volume enclosing the current distribution. MKS units are used throughout this report, and symbols such as μ_o, ϵ_o, ϵ_r, E, H, B, D, etc., are as usually defined in modern textbooks.[7,8,9] The wavy line under a symbol denotes the symbol to be a vector quantity.

In the case of a small conducting loop carrying a current I, Eq. 3-1 reduces to the following simple formula:

$$m = AI \tag{3-2}$$

where A is the area of the loop. The direction of the dipole is perpendicular to the plane of the loop. Equation 3-2 is commonly used as the definition of a magnetic dipole.[8]

Equation 3-1 can be applied to the case of a dielectric resonator, even though a real flow of electric current does not occur. The following equation of Maxwell shows that the displacement current $j\omega\underset{\sim}{D}$ and the electric current $\underset{\sim}{\imath}$ are interchangeable insofar as excitation of magnetic field is concerned.

$$\nabla \times H = \underset{\sim}{\imath} + j\omega\underset{\sim}{D} \tag{3-3}$$

Therefore, $j\omega\underset{\sim}{D} = j\omega\varepsilon\underset{\sim}{E}$ may be substituted for $\underset{\sim}{\imath}$ in Eq. 3-1 as follows

$$\underset{\sim}{m} = \frac{j\omega\varepsilon_o}{2}\iiint \varepsilon_r \underset{\sim}{R}\times\underset{\sim}{E}\, dv \tag{3-4}$$

If the electric field function of a given dielectric-resonator mode is known, the magnetic dipole moment may be computed from Eq. 3-4. Since E of the resonant mode exists outside of the dielectric body as well as inside, the integration rigorously should be performed

over the infinite outside volume in addition to the internal volume. Fortunately, the external electric field is less effective than the internal field by the factor $1/\varepsilon_r \approx 1/100$, and furthermore it decays rapidly with distance. Thus, the contribution to m of the external electric field is very small.

A cylindrical resonator body and the fundamental circular electric mode, $TE_{01\delta}$, will now be assumed. With reference to Figure 3-2, the electric field vector is in the $\underset{\sim}{\theta}$ direction, and is a function only of r and z. By symmetry considerations, m has the direction of z, and thus Eq. 3-4 becomes

$$m = \frac{j\omega\varepsilon_o}{2} \iiint \varepsilon_r r\, E_\theta\, r\, d\theta\, dr\, dz$$

or, after integrating from $\theta = 0$ to 2π,

$$m = j\pi\omega\varepsilon_o \iint \varepsilon_r r^2 E_\theta\, dr\, dz \qquad (3\text{-}5)$$

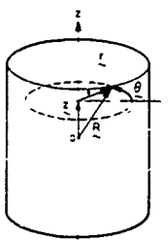

Figure 3-2. Coordinate System for Dielectric Cylinder

Before Eq. 3-5 can be evaluated, E_θ as a function of r and z must be known. Because the exact function is not known and cannot feasibly be calculated, the second-order solution will be used as an approximation. This approximation assumes the cylindrical dielectric body to be enclosed in an infinitely long magnetic-wall waveguide having the same cross section as the dielectric body (Figure 3-3). For the fundamental $TE_{01\delta}$ mode of resonance, the fields in this boundary are completely represented by propagating TE_{01} waves in the dielectric section and attenuating TE_{01} waves

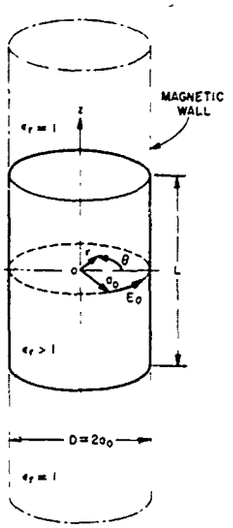

Figure 3-3. Dielectric Cylinder in Magnetic-wall Waveguide Boundary

in the air regions. This TE_{01} mode in a magnetic-wall waveguide is related by duality to the TM_{01} mode in an electric-wall waveguide, that is, E in the first case is proportional to H in the second case. Since the second case is well known, E_θ of the TE_{01} mode in a magnetic-wall waveguide may be written at once as follows:

$$E_\theta = E_o f(z) \frac{J_1(k_c r)}{J_1(p_{01})} \text{ for } 0 \le r \le a_o, \; E_\theta = 0 \text{ for } r > a_o \qquad (3\text{-}6)$$

$$k_c = \frac{p_{01}}{a_o} = \frac{2p_{01}}{D} \qquad (3\text{-}7)$$

and p_{01} is the first positive root of

$$J_0(p_{01}) = 0 \qquad (3\text{-}8)$$

Therefore,

$$p_{01} = 2.405 \qquad (3\text{-}9)$$

The function f(z) is as follows in the dielectric region

$$f(z) = \cos \beta_d z \quad \text{for } \frac{-L}{2} \le z \le \frac{L}{2} \qquad (3\text{-}10)$$

and as follows in the air regions

$$f(z) = \cos\frac{\xi_d L}{2} \cdot e^{-\alpha_a(|z|-L/2)} \quad \text{for } |z| \geq \frac{L}{2} \tag{3-11}$$

Equations 3-10 and 3-11 provide the necessary continuity of f(z) at $z = \pm L/2$. Note that E_o is the electric field value at $r = a_o$, $z = 0$.

Equations 3-5 and 3-6 give

$$m = \frac{j2\pi\omega\epsilon_o E_o}{J_1(p_{01})} \int_{z=0}^{\infty} \epsilon_r f(z)\, dz \int_{r=0}^{a_o} r^2 J_1(\kappa_c r)\, dr \tag{3-12}$$

Symmetry allows integration with respect to z to extend from $z = 0$ to ∞ instead of $-\infty$ to ∞. A factor of [illegible] has been inserted to compensate for this change. In the direction of [illegible] is extended only to $r = a_o$, since the second-order solution assumes zero fields for $r > a_o$.

The following integral is obtained from Jahnke and Emde, p. 145 [10]

$$\int x^2 J_1(x)dx = x^2 J_2(x) \tag{3-13}$$

Therefore,

$$\int_0^{a_o} r^2 J_1(\kappa_c r)\, dr = \frac{a_o^2}{\kappa_c} J_2(\kappa_c a_o) = \frac{a_o^3}{p_{01}} J_2(p_{01}) \tag{3-14}$$

where Eq. 3-7, $p_{01} = \kappa_c a_o$, was used. Now apply the following recursion formula (Jahnke and Emde p. 144)

$$J_{n+1}(x) = \frac{2n}{x} J_n(x) - J_{n-1}(x) \tag{3-15}$$

therefore,

$$J_2(p_{01}) = \frac{2}{p_{01}} J_1(p_{01}) - J_0(p_{01}) = \frac{2}{p_{01}} J_1(p_{01}) \tag{3-16}$$

since $J_0(p_{01}) = 0$ by definition of p_{01}.

Equations 3-12, 3-14, and 3-16 yield

$$m = \frac{j4\pi a_o^3 \varepsilon_o E_o}{(p_{01})^2} \int_0^\infty \varepsilon_r f(z)\, dz \tag{3-17}$$

Now use the following relations

$$\eta = \sqrt{\frac{\mu_o}{\varepsilon_o}} = 120\pi \tag{3-18}$$

$$k\varepsilon_o = \frac{2\pi}{\lambda} \cdot \frac{1}{\eta} = \frac{1}{60\lambda} \tag{3-19}$$

Thus,

$$m = \frac{\pi a_o^3 E_o}{15(p_{01})^2 \lambda} \int_0^\infty \varepsilon_r f(z)\, dz \tag{3-20}$$

Integration of the $f(z)$ functions given by Eqs. 3-10 and 3-11 is straightforward. The result is as follows with $\varepsilon_r = 1$ in the $z = L/2$ to ∞ region.

$$m = \frac{\pi D^3 L \varepsilon_r E_o}{240(p_{01})^2 \lambda} \left[\frac{2}{\varepsilon_d L} \sin \frac{\varepsilon_d L}{2} + \frac{2}{\varepsilon_r \varepsilon_d L} \cos \frac{\varepsilon_d L}{2} \right] \tag{3-21}$$

Note that when $\varepsilon_d L/2$ is small and ε_r is large, the quantity within the brackets approaches unity.

c. Stored Energy

At resonance, the instantaneous peak values of magnetic stored energy W_m and electric stored energy W_e are equal. (The equality of magnetic and electric energies is often used to define resonance.) These energy quantities may be computed from

$$W_m = \frac{\mu_o}{2} \iiint H^2 \, dv \tag{3-22}$$

and

$$W_e = \frac{\varepsilon_o}{2} \iiint \varepsilon_r E^2 \, dv \tag{3-23}$$

where integration is performed inside and outside the dielectric resonator body. The material is assumed here to be nonmagnetic that is, $\mu = \mu_o$ in both regions. Since W_m and W_e are equal at resonance, either Eqs. 3-22 and 3-23 may be used for the stored energy computation. Equation 3-23 is preferred, since the high value of ε_r results in most of the electric energy being inside the dielectric body, where the field function is known to a rather good approximation. The magnetic field on the other hand has a much larger proportion of its energy outside the body, so that calculation of Eq. 3-22 will be less accurate.

Equation 3-23 will now be evaluated assuming the zero-order electric field functions given by Eqs. 3-6, 3-7, and 3-8. We obtain

$$W_e = \frac{2\pi\varepsilon_o E_o^2}{\left[J_1(p_{01})\right]^2} \int_{z=0}^{\infty} \varepsilon_r \left[f(z)\right]^2 dz \int_{r=0}^{a_p} r \left[J_1(\kappa_c r)\right]^2 dr \tag{3-24}$$

The Bessel function integral may be evaluated from the following relation given by Jahnke and Emde, p. 146.[10]

$$\int x\left[J_1(\alpha x)\right]^2 dx = \frac{x^2}{2}\left\{\left[J_1(\alpha x)\right]^2 - J_0(\alpha x)\, J_2(\alpha x)\right\} \qquad (3\text{-}25)$$

Therefore,

$$\int_0^{a_o} r\left[J_1(k_c r)\right]^2 dr = \frac{a_o^2}{2}\left\{\left[J_1(p_{01})\right]^2 - J_0(p_{01})\, J_2(p_{01})\right\} \qquad (3\text{-}26)$$

$$= \frac{a_o^2}{2}\left[J_1(p_{01})\right]^2 \qquad (3\text{-}27)$$

where Eq. 3-26 reduces to Eq. 3-27, since $J_0(p_{01}) = 0$.

Hence,

$$W_e = \pi a_o^2 \varepsilon_o E_o^2 \int_0^{\infty} \varepsilon_r \left[f(z)\right]^2 dz \qquad (3\text{-}28)$$

Straightforward integration utilizing the assumed f(z) functions given by Eqs. 3-10 and 3-11 yields

$$W_e = \frac{1}{8}\varepsilon_o \varepsilon_r \pi D^2 L E_o^2 \left[\frac{1}{2}\left(1 + \frac{\sin \varepsilon_d L}{\varepsilon_d L}\right) + \frac{\cos^2(\varepsilon_d L/2)}{\varepsilon_d - \varepsilon_r}\right]$$

As in Eq. 3-21, the quantity within the brackets approaches unity for $\varepsilon_d L$ small and ε_r large. It is interesting to note in this case that W_e is simply $\frac{1}{2}\varepsilon E_o^2$ times the volume of the dielectric cylinder

d. Generalized Coupling Between Magnetic Dipoles

A generalized formula for the coupling coefficient between two magnetic dipole resonators will now be derived. The resonators will be represented by conducting loops in an arbitrary enclosure, as shown in Figure 3-4. The loops have an inductance L and are resonated at f_o by series capacitors C, where $f_o = 1/2\pi\sqrt{LC}$. The magnetic dipole moment of Loop 1 in Figure 3-4 is given by Eq. 3-2 as follows

$$m_1 = AI_1 \qquad (3\text{-}30)$$

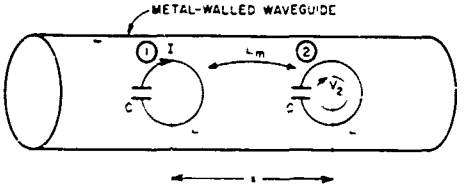

Figure 3-4. Coupled Resonant Loops in Arbitrary Waveguide Enclosure

where A is the loop area, I the current, and where the subscript 1 denotes Loop 1. The magnetic stored energy is

$$W_{m1} = \frac{1}{2} L I_1^2 \qquad (3\text{-}31)$$

Let L_m be the mutual inductance between the loops, and V_2 the induced voltage in Loop 2 due to I_1 in Loop 1. Then, by definition of mutual inductance,

$$V_2 = j\omega L_m I_1 \qquad (3\text{-}32)$$

The induced voltage V_2 is also given by the following electromagnetic integral relationship

$$V_2 = -\oint \underline{E}_2 \cdot d\underline{\ell} = j\omega \iint \underline{B}_2 \cdot d\underline{a} = j\omega\mu_o \iint \underline{H}_2 \cdot d\underline{a} \qquad (3\text{-}33)$$

where $\underline{B}_2$ and $\underline{H}_2$ are field values in Loop 2 due to the current in Loop 1. The line integral is evaluated over a closed path along the loop conductor

and through the capacitor. The surface integral is evaluated over the area of the loop. Now, let $\underset{\sim}{H}_2$ be a mean value in the loop area, A. (For small loops, $\underset{\sim}{H}_2$ can be taken to be the value at the center of the loop.) Then

$$V_2 = j\omega\mu_o \underset{\sim}{H}_2 \cdot \underset{\sim}{A} \tag{3-34}$$

Now combine Eqs. 3-31 and 3-32 as follows

$$k = \frac{L_m}{L} = \frac{V_2 I_1}{j2\omega W_{m1}} \tag{3-35}$$

where the coupling coefficient k is equal to L_m/L by definition of coupling coefficient. Next substitute Eqs. 3-30 and 3-34 into 3-35 and obtain

$$k = \frac{\mu_o \underset{\sim}{H}_2 \cdot \underset{\sim}{m}_1}{2W_{m1}} \tag{3-36}$$

This formula for the coupling coefficient between two resonant magnetic dipoles applies in general, although derived for a pair of simple loops. The magnetic dipoles can be of any type in any environment including free space.

e. Excitation of a Waveguide by a Magnetic Dipole

The general coupling formula, Eq. 3-36, will be particularized to the case of a pair of identical magnetic dipoles in a waveguide. The notation will follow Collin,[7] p. 201-204. Thus, the E field of a given waveguide mode is given by

$$\underset{\sim}{E}_p^{\pm} = (\underset{\sim}{e}_p \pm \underset{\sim}{e}_{zp}) e^{\mp \gamma_p z} \tag{3-37}$$

where subscript p indicates the type and order of the mode (e.g., TE_{10}, TE_{11}, TM_{11}, etc.), $\underset{\sim}{e}_p$ is the transverse component of field, $\underset{\sim}{e}_{zp}$ is the longitudinal component of field, γ_p is the propagation constant, and $\pm$ denotes the direction of propagation of the wave (+ applies to the +z direction and -- to the -z direction). In a similar manner,

$$\underset{\sim}{H}_p^{\pm} = (\pm \underset{\sim}{h}_p + \underset{\sim}{h}_{zp})\, e^{\mp \gamma_p z} \tag{3-38}$$

The following power normalization relationship applies to $\underset{\sim}{e}_p$ and $\underset{\sim}{h}_p$ of each mode.

$$\iint \underset{\sim}{e}_p \times \underset{\sim}{h}_p \cdot d\underset{\sim}{a} = 1 \tag{3-39}$$

where integration is over the transverse cross section of the waveguide.

The total fields are given by the following infinite summations over all possible modes

$$\underset{\sim}{E}^+ = \sum_p a_p \underset{\sim}{E}_p^+ \quad , \quad \underset{\sim}{H}^+ = \sum_p a_p \underset{\sim}{H}_p^+ \tag{3-40}$$

$$\underset{\sim}{E}^- = \sum_p b_p \underset{\sim}{E}_p^- \quad \underset{\sim}{H}^- = \sum_p b_p \underset{\sim}{H}_p^- \tag{3-41}$$

where a_p and b_p are amplitude factors of waves in the +z and -z directions, respectively.

Now assume a magnetic dipole of moment $\underset{\sim}{m}$ having arbitrary orientation and arbitrary location in the z = 0 transverse plane. Collin[7] on p 204 gives the following amplitudes for the waves of type and order p excited by the magnetic dipole

$$a_p = \frac{j\omega\mu_o}{2} \underset{\sim}{H}_p^- \cdot \underset{\sim}{m} \tag{3-42}$$

$$b_p = \frac{j\omega\mu_o}{2} \underset{\sim}{H}_p^+ \cdot \underset{\sim}{m} \tag{3-43}$$

where $\underset{\sim}{H}_p^-$ and $\underset{\sim}{H}_p^+$ are normalized magnetic fields of mode p as defined by Eqs. 3-38 and 3-39.

Equations 3-42 and 3-43 give the amplitude of each mode excited by the magnetic dipole. In the present case of interest, all modes attenuate along the waveguide, that is, $\gamma_p = \alpha_p + j0$ for all p. In the rectangular waveguide geometry of Figure 3-1, the following modes have $\underset{\sim}{H}$ components in the direction of $\underset{\sim}{m}$ and therefore are excited by $\underset{\sim}{m}$: TE_{10}, TE_{30}, TE_{12}, TE_{32}, TM_{12}, TM_{32}, etc. Of these modes, the TE_{10} mode has the lowest cut-off frequency, and therefore the lowest attenuation constant. Thus, at a sufficient longitudinal distance from the magnetic dipole, the total field may be represented with sufficient accuracy by the TE_{10} mode field. The assumption will now be made that only the TE_{10} mode need be considered. In a later report, other modes will be added to the analysis, in order to improve the accuracy of the coupling formula for close spacing.

Collin[7] on p. 299 gives the following normalized x-directed field component for the TE_{10} mode.

$$h_x = \left(\frac{2}{jab\pi\eta}\right)^{\frac{1}{2}} \sin\frac{\pi x_1}{a} \tag{3-44}$$

where $\eta = \sqrt{\mu_o/\epsilon_o} = 120\pi$ ohms, and

$$\gamma = \alpha = \frac{\pi}{a}\sqrt{1 - \left(\frac{f}{c}\right)^2} \tag{3-45}$$

In Eqs. 3-44 and 3-45 and in the following analysis, h_x, Γ, and α apply to the TE_{10} mode, and a and b are the dimensions of the waveguide, as shown in Figure 1. The dimension x_1 is the distance from a side wall of the waveguide to the center of the magnetic dipole, and will be assumed equal to a/2.

Equation 3-42 gives the amplitude of the forward-directed TE_{10} wave excited by an x-oriented magnetic dipole m at z = 0, x = a/2, as follows

$$a_{TE10} = -\frac{\omega\mu_o m_1}{2}\left(\frac{j\lambda\alpha}{ab\pi\eta}\right)^{\frac{1}{2}} \tag{3-46}$$

The TE_{10} mode H_x field at z = s may now be obtained from Eqs. 3-38, 3-40, 3-44, and 3-46, noting that $\omega\mu_o\lambda/\eta = 2\pi$.

$$H_{x2} = a_{TE10}\, h_x\, e^{-\alpha s} = -\frac{2m_1}{ab}\, e^{-\alpha s} \tag{3-47}$$

This will be substituted in Eq. 3-36, yielding the following formula for TE_{10}-mode coupling between two resonant x-directed magnetic dipoles on the center-line of a rectangular waveguide

$$k = \left(\frac{2e^{-\alpha s}}{ab}\right)\left(\frac{-\mu_o m_1^2}{2W_{m1}}\right) \tag{3-48}$$

Subscript 1 on m_1 and W_{m1} implies that m and W_m of the resonant magnetic dipole are evaluated for the same amplitude of excitation of the dipole. Note that the actual amplitude of excitation does not matter, since it cancels out when the ratio m_1^2/W_{m1} is taken.

The first factor in Eq. 3-48 depends only on the constants of the waveguide and on the center-to-center spacing s. The second

factor depends only on the constants of the magnetic dipole resonators. Before evaluating the second factor in explicit terms, it will be instructive to consider the factor's basic nature. Let $W_{m1} = W_{e1}$ at resonance, and use Eqs. 3-4 and 3-23. Thus

$$\frac{\mu_o m_1^2}{2W_{m1}} = -\frac{\pi^2}{\lambda^2} \frac{\left| \iiint \epsilon_r \underline{R} \times \underline{E} \, dv \right|^2}{\iiint \epsilon_r E^2 \, dv} \tag{3-49}$$

Now let $E = E_\theta$, where E_θ is a function of r and z, and is independent of θ.

$$\frac{\mu_o m_1^2}{2W_{m1}} = -\frac{2\pi^3}{\lambda^2} \frac{\left[\iint \epsilon_r r^2 E_\theta \, dr \, dz \right]^2}{\iint \epsilon_r r E_\theta^2 \, dr \, dz} \tag{3-50}$$

Examination of either Eq. 3-49 or 3-50 indicates that the computation of $\mu_o m_1^2 / 2W_{m1}$ is likely to be relatively unaffected by deviations of E from the true E function. In fact, these equations have the general form of variational expressions in which first-order errors in E produce only second order errors in the quantity computed. It is not yet known whether either Eq. 3-49 or 3-50 has this variational property but a preliminary study shows that at least a quasi-variational characteristic exists. Thus, the use of the approximate E_θ function given by Eqs. 3-6, 3-10, and 3-11 should yield good results in the computation of the coupling coefficient.

f. Coupling Coefficient Between Dielectric Resonators

Equation 3-21 for m and Eq. 3-49 for $W_e = W_m$ may now be substituted in Eq. 3-48, letting $\pi^3/(p_{01})^4 = \pi^3/2.405^4 = 0.927$.

$$k = \frac{0.927D^4L\epsilon_r\alpha e^{-\alpha s}}{ab\lambda_o^2} \left\{ \frac{\left[\frac{2}{\beta_d L}\sin\frac{\beta_d L}{2} + \frac{2}{\epsilon_r\alpha_a L}\cos\frac{\beta_d L}{2}\right]^2}{\frac{1}{2}\left(1 + \frac{\sin\beta_d L}{\beta_d L}\right) + \frac{\cos^2(\beta_d L/2)}{\epsilon_r\alpha_a L}} \right\} \quad (3\text{-}51)$$

In this formula for coupling coefficient, λ_o is the measured resonant wavelength ($\lambda_o = c/f_o$) of the resonators. (Measurements reported in the next section show that better accuracy results from use of the measured λ_o value rather than the value computed from the second-order solution.) The second-order equations of the First Quarterly Report[1] should be used in evaluating B_d and α_a.

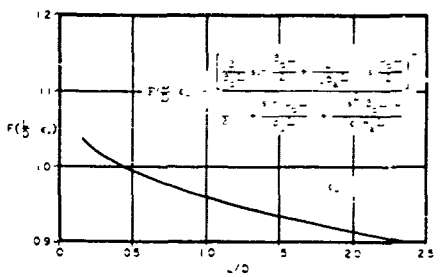

Figure 3-5. Graph of Quantity Within Braces in Eq. 3-51, $\epsilon_r = 100$

The quantity within the braces in Eq. 3-51 is approximately equal to unity. This quantity, as computed by means of the second-order solution, is a function of the dielectric constant ϵ_r and the dimensional ratio L/D of the dielectric resonator. Figure 3-5 shows a plot of the braced quantity versus L/D for the case $\epsilon_r = 100$. It is seen that the [illegible] unity for L/D between 0.2 and 0.[illegible], which is believed to include the most practical range of L/D for oscillator purposes. Over the wider range L/D = 0.15 to 1.0, the deviation from unity is within ±4 per cent.

Thus, to a good approximation,

$$k = \frac{0.927D^4L\epsilon_r\alpha e^{-\alpha s}}{ab\lambda_o^2}, \quad 0.25 \le L/D \le 0.7 \quad (3\text{-}52)$$

Equation 3-52 has adequate accuracy for usual filter design purposes. If desired, the quantity $F(L/D, \varepsilon_r)$ plotted in Figure 3-5 may be applied to Eq 3-52 as a correction factor, thus yielding the greater accuracy of Eq. 3-51. The plotted function $F(L/D, \varepsilon_r)$ applies to $\varepsilon_r = 100$, but holds quite well for widely different ε_r values.

4. Measurement of Coupling Between Resonators

A series of measurements have been made of the coupling coefficient k between a pair of identical dielectric resonators arranged along the center line of a cut-off waveguide. The geometry is that of Figures 3-1 and 4-1. Two different sizes of resonators were used as follows:

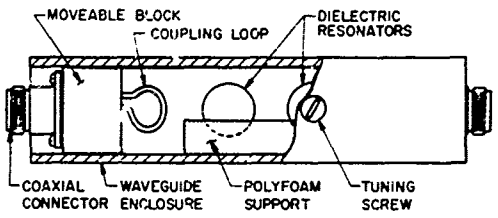

Figure 4-1. Typical Test Fixture for Measurement of Coupling Coefficient Between Dielectric Resonators

Pair No. 1	Pair No. 2
D = 0.3930	D = 0.3930
L = 0.1600	L = 0.2500
L/D = 0.407	L/D = 0.636

The resonators were ground within a tolerance of ±0.0002 on diameter and length. The material was from the series of samples measured during the first quarter. The frequencies and unloaded Q values of this series of samples are given in the First Quarterly Report[1] in Figure 2-5 and Table 3-2. As described in Section 2 of the present report, other pieces from the same series were measured to have $\varepsilon_r = 97.6$.

The three aluminum waveguides are dimensioned internally as follows:

WG No. 1	WG No. 2	WG No. 3
a = 0.750"	a = 0.995"	a = 0.625"
b = 0.750	b = 0.995	b = 1.374

Six sets of coupling data were obtained from the two pairs of resonators and three sizes of waveguides. In each case, the resonators were supported along the center line of the waveguide by means of polyfoam, as shown in Figures 4-1 and 4-2. Slots were milled in the polyfoam pieces to support the resonant disks along the waveguide center lines. The resonator pairs were excited by coupling loops at the ends of coaxial lines, as shown in Figure 4-1. The loops were mounted on metal blocks machined to fit the inside dimensions of each waveguide.

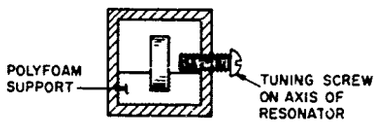

Figure 4-2 Method of Supporting and Tuning the Dielectric Resonators

A band-pass filter consisting of a pair of resonators yields a transmission response having two peaks when the resonators are over-coupled; that is, when k is greater than k_c, where k_c is the critical coupling yielding a maximally flat response. The transmission curve sketched in Figure 4-3 shows the typical shape of the peaks, and defines the parameters associated with the response. The coupling coefficient k may be computed from the center frequency f_o, the peak separation Δf, and the transmission dip ΔL (in db) by means of the following relations:

$$k = \frac{1}{\sqrt{1 - \left(\frac{k_c}{\kappa}\right)^2}} \cdot \frac{\Delta f}{f_o} \qquad (4\text{-}1)$$

$$\Delta L = 20 \log_{10} \left[\frac{1}{2} \left(\frac{k}{k_c} + \frac{k_c}{k} \right) \right] \text{db} \qquad (4\text{-}2)$$

The factor

$$f(\Delta L) = \frac{1}{\sqrt{1 - \left(\frac{k_c}{k} \right)^2}} \qquad (4\text{-}3)$$

is plotted as a function of ΔL in Figure 4-3. Note that this factor is near unity, deviating from unity by less than 0.5% for $\Delta L > 14$ db. By means of Figure 4-3 and measured values of Δf and f_o, k was obtained for various center-to-center spacings of the resonators. The loop couplings were purposely weak so as to maximize ΔL, thus sharpening the peaks and making the measurement less sensitive to ΔL. At the largest values of s for which measurements were taken, ΔL had diminished to about 3.0 db, and the factor was about 1.1. However, the care of measurement was such that deterioration of accuracy is not noticeable in these cases.

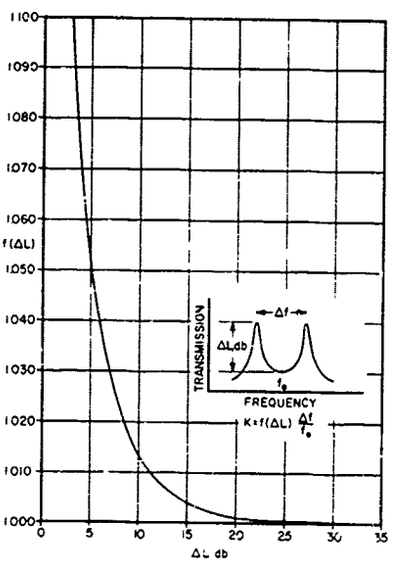

Figure 4-3. Graph of Factor f(ΔL) Used in Measurement of Coupling Coefficient Between Two Resonators

When making the coupling measurement, the resonant frequencies of the two resonators must be identical. The frequencies of corresponding resonators differed by about 0.5 per cent, which was

excessive for the coupling measurement. It was found that a resonator could be conveniently tuned by means of a screw introduced from a side wall of the waveguide on the axis of the resonator. The predominant field in this region is magnetic. The effect of the screw is t reduce the stored magnetic energy of the resonant mode, thus raising the resonant frequency. This is opposite to the usual effect of a tuning screw in a cavity, which acts to increase the electric stored energy, and thereby lower the resonant frequency. In order to achieve an adequate effect on the magnetic stored energy, the screw must be relatively large. A quarter-inch diameter screw was found to be properly proportioned for the 0.4-inch-diameter dielectric resonators. For example, with this size screw, the resonant frequency was increased by one per cent when the end of the screw was spaced about 0.15 inch from the resonator. The procedure used in obtaining the coupling data was to tune the resonator having the lowest resonant frequency so that the frequency spacing betwe·n the pair of peaks was minimized, thus assuring synchronous tuning.

The measured values of k versus s for the six cases are plotted in Figure 4-4. The measured points fall along smooth curves that can be used for design purposes. At other center frequencies, all dimensions should be scaled proportional to λ_o. However, design use of Figure 4-4 requires that ε_r be in the vici·ity of 97.6, for example, in the range 90 to 105. A g·ne·al design f·r.ula is clearly needed in view of the restriction placed on dielectric constant and geometry and the impracticability of obtaining data for all useful situations.

The coupling formula, Eq. 3-51, has been evaluated for the six cases of Figure 4-4, utilizing the respective dimensions and center frequencies, and $\varepsilon_r = 97.6$. The formula is plotted for each case in Figure 4-5, with the exp·· mental points shown for comparison.

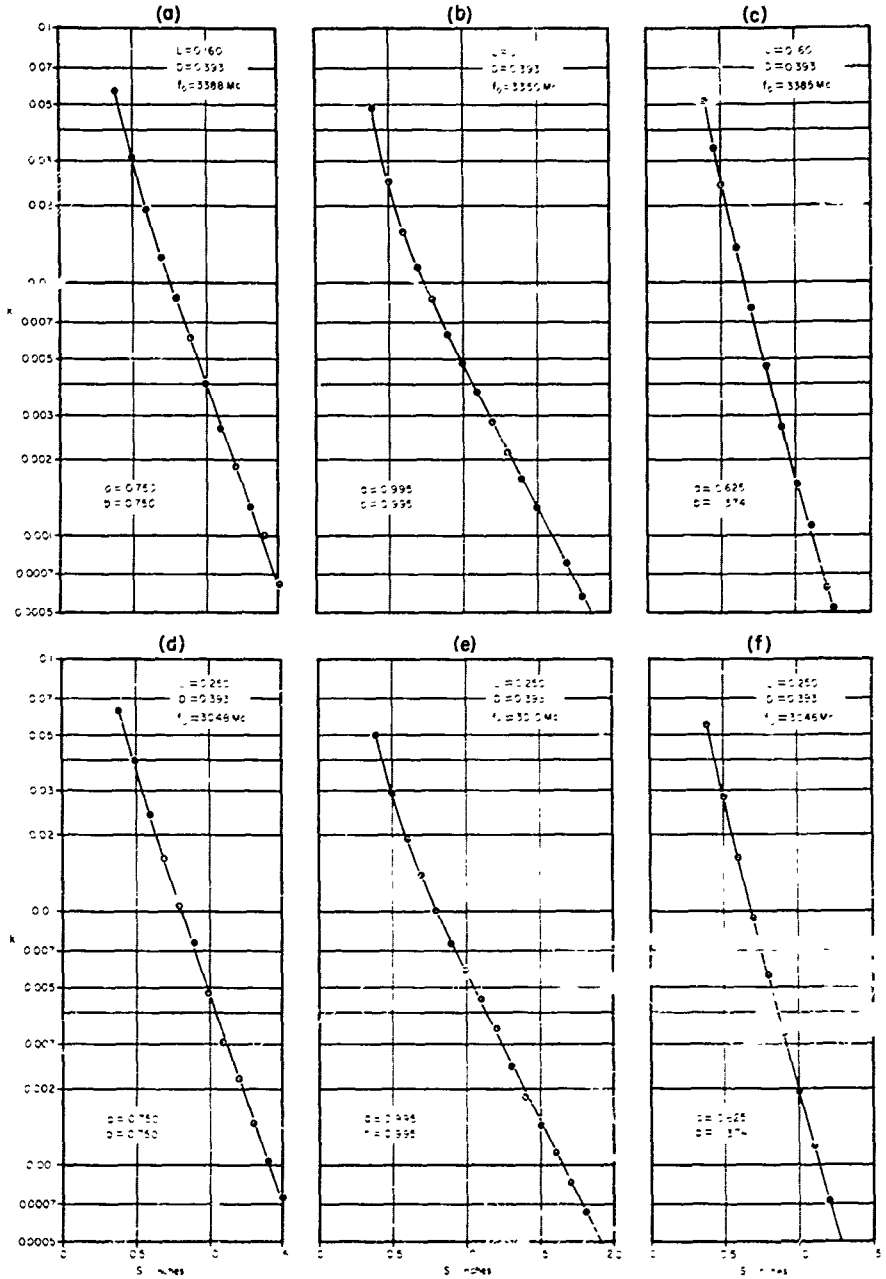

Figure 4-4. Measured Curves of κ Versus s for Various Resonator and Enclosure Dimensions

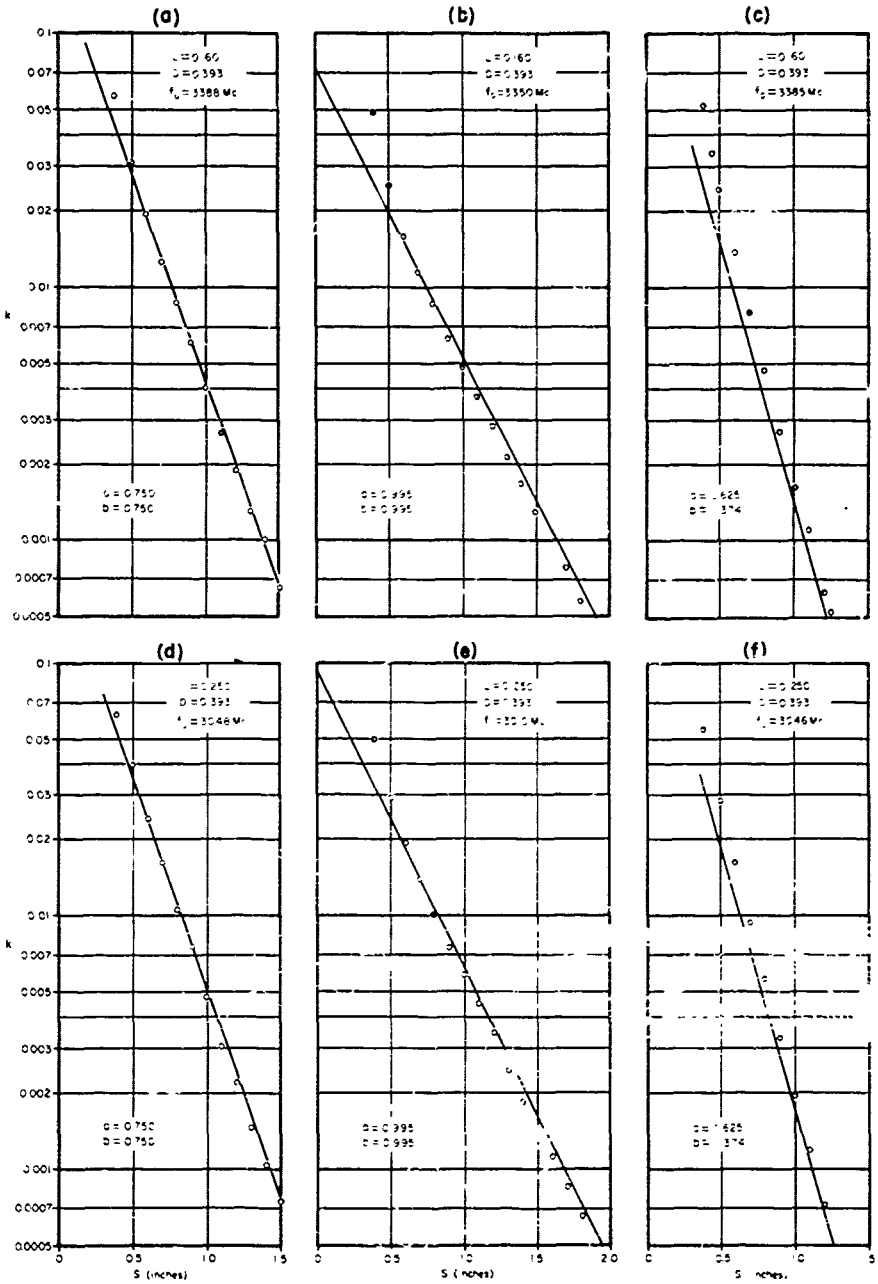

Figure 4-5. Comparison of Experimental and Theoretical Coupling Coefficient Data

The computed curves are straight lines on a semi-log graph, with the slope determined by α, the waveguide attenuation of the TE_{10} mode. The experimental data is seen in each case to have the correct slope when the center-to-center spacing s exceeds roughly 0.75 times the larger of either a or b. This behavior is to be expected, since for larger s the TE_{10} mode predominates, while for smaller s higher mode coupling contributes significantly to total coupling. In the region of s greater than about 0.75 times the larger of a or b, the measured and calculated coupling-coefficient curves agree within about ±10 per cent. The theoretical values are in some cases higher than the measured values, and in other cases lower. This amount of discrepancy compares very favorably with that occurring in applications of small-aperture theory to filter design. The accuracy of Eq. 3-51 is considered adequate for ordinary design purposes, when s exceeds 0.75 a and 0.75 b.

For L = 0.160 inch the simplified coupling formula, Eq. 3-52, yields values essentially the same as those from Eq. 3-51, while for L = 0.250 inch Eq. 3-52 is about 1.7 per cent higher than Eq. 3-51. (These differences are obtained immediately from Figure 3-5, in which the ratio of the two equations is plotted.) The general direction of the difference is such that the disagreement between measurement and theory is greater for the simplified formula than for the more complex formula. However, the additional 1.7 per cent error is not likely to be significant in most practical design applications.

SECTION V

CONCLUSIONS

Air gaps of even 0.0001 inch can cause serious errors in the measurement of high dielectric constant. Two methods were perfected that are insensitive to air gaps. This insensitivity results from the use of modes having zero electric field at dielectric surfaces adjacent to metal walls. The measurement accuracy is at least within 1 per cent. These methods utilize cylindrical dielectric samples that can be the actual resonators of a filter. The two methods should have wide general utility for the measurement of high dielectric constant materials.

Measurements on one batch of dielectric samples obtained from American Lava Corp. indicated a variation of dielectric-constant values that correlated very well with the densities of the individual samples. Dielectric constant values obtained for several Signal Corps samples confirmed the supposition in the First Quarterly Report that the second-order solution yields resonant frequencies about 10 per cent too low.

It has been found feasible to calculate the magnetic dipole moment and stored energy of dielectric resonators. In terms of these and other basic parameters, a useful coupling coefficient formula has been derived. The formula yields values within ±10 per cent of measured data in its range of validity. At present the formula is not accurate in the case of close spacings. However, an extension of the analysis is believed feasible to improve that situation.

SECTION VI

PROGRAM FOR NEXT INTERVAL

Further work will be done on the two methods of dielectric-constant measurement in order to resolve their minor disagreement, and to define more precisely their sources of error.

The theoretical analysis will be extended to include higher-mode terms. Also, other useful coupling configurations will be treated.

Measurements will be made on a series of one- and two-resonator band-pass filters in order to determine the effect of waveguide-wall proximity on the effective unloaded Q values. The data will indicate the smalle allowable dimensions of the metallic enclosure. and hence the minimum feasible volume of a complete dielectric-resonator filter. Certain practical problems relating to filter construction will be explored.

SECTION VII

LIST OF REFERENCES

1. S. B. Cohn and C. W. Chandler, "Investigation of Microwave Dielectric-Resonator Filters," First Quarterly Report on Contract DA-36-039-AMC-02267(E), 1 July 1963 to 30 September 1963, Rantec Corp., Project No. 31625.

2. N. Marcuvitz, "Waveguide Handbook," pp. 18, 28, 69-71, McGraw-Hill Book Co., New York, 1951.

3. N. Marcuvitz, Op. Cit., pp. 18, 31-33, 41-43, 46, 92-93.

4. S. B. Cohn, "Direct-Coupled-Resonator Filters," Proc. IRE, Vol. 45, pp. 187-196, February 1957.

5. "Reference Data for Radio Engineers," 4th Edition, ITT Corp., New York, 1956, pp. 218-221.

6. A. Okaya and L. F. Barash, "The Dielectric Microwave Resonator," Columbia Radiation Laboratory Report, Columbia University, New York, N. Y. Also, Proc. IRE, Vol. 50, pp. 2081-2090, Oct. 1962

7. R. E. Collin, "Field Theory of Guided Waves," McGraw-Hill, New York, 1960.

8. E. C. Jordan, "Electromagnetic Waves and Radiating Systems," Prentice-Hall, Inc., New York, 1950.

9. S. Ramo and J. R. Whinnery, "Fields and Waves in Modern Radio," 2nd Edition John Wiley and Sons, Inc. New York, 1953.

10. E. Jahnke and F. Emde, "Tables of Functions," Dover Publications, New York, 1943.

SECTION VIII

IDENTIFICATION OF KEY TECHNICAL PERSONNEL

	Hours
Dr. Seymour B. Cohn Specialist	104
Mr. Charles W. Chandler Senior Engineer	20
Mr. Kenneth C. Kelly Senior Engineer	131
Mr. Richard V. Reed Engineer	50

AD DIV

Rantec Corporation, Calabasas, California

MICROWAVE DIELECTRIC-RESONATOR FILTERS, by S. B. Cohn and K. C. Kelly, an investigation. Second Quarterly Report, 1 October to 31 December 1963, 45p. incl. illus. tables, 10 refs. (rept. no. 2, proj. 31625) (Contract DA 36-039-AMC-02267(E) uncl.

The serious effect of air gaps on the measurement of high dielectric-constant values is discussed. Two measurement techniques are described in which air gaps are made to be insignificant sources of error. Data obtained by these methods are presented and shown to be consistent at least within 1 per cent.

(over)

UNCLASSIFIED

1 Dielectric-Resonator Filters -- Analyses
I. Title Microwave Dielectric-Resonator Filters
II Cohn, S. B and Kelly, K. C.
III Rantec Corp., Calabasas, Calif.
IV. Contract DA 36-039-AMC-02267(E)

UNCLASSIFIED

AD DIV

Rantec Corporation, Calabasas, California

MICROWAVE DIELECTRIC-RESONATOR FILTERS, by S. B. Cohn and K. C. Kelly, an investigation. Second Quarterly Report, 1 October to 31 December 1963, 45p. incl. illus. tables, 10 refs. (rept. no. 2, proj. 31625) (Contract DA 36-039-AMC-02267(E) uncl.

The serious effect of air gaps on the measurement of high dielectric-constant values is discussed. Two measurement techniques are described in which air gaps are made to be insignificant sources of error. Data obtained by these methods are presented and shown to be consistent at least within 1 per cent.

(over)

UNCLASSIFIED

1. Dielectric-Resonator Filters -- Analyses
I. Title Microwave Dielectric-Resonator Filters
II. Cohn, S. B and Kelly, K. C
III Rantec Corp., Calabasas, Calif
IV Contract DA 36-039-AMC-02267(E)

UNCLASSIFIED

AD DIV

Rantec Corporation, Calabasas, California

MICROWAVE DIELECTRIC-RESONATOR FILTERS, by S. B. Cohn and K. C. Kelly, an investigation. Second Quarterly Report, 1 October to 31 December 1963, 45p. incl. illus. tables, 10 refs. (rept. no. 2, proj. 31625) (Contract DA 36-039-AMC-02267(E) uncl.

The serious effect of air gaps on the measurement of high dielectric-constant values is discussed. Two measurement techniques are described in which air gaps are made to be insignificant sources of error. Data obtained by these methods are presented and shown to be consistent at least within 1 per cent.

(over)

UNCLASSIFIED

Dielectric-Resonator Filters -- Analyses
Title Microwave Dielectric-Resonator Filters
1 Cohn, S. B and Kelly, K. C
II Rantec Corp., Calabasas, Calif
Contract DA 36-039-AMC-02267(E)

UNCLASSIFIED

AD DIV

Rantec Corporation, Calabasas, California

MICROWAVE DIELECTRIC-RESONATOR FILTERS, by S. B. Cohn and K. C. Kelly, an investigation. Second Quarterly Report, 1 October to 31 December 1963, 45p. incl. illus. tables, 10 refs. (rept. no. 2, proj. 31625) (Contract DA 36-039-AMC-02267(E) uncl.

The serious effect of air gaps on the measurement of high dielectric-constant values is discussed. Two measurement techniques are described in which air gaps are made to be insignificant sources of error. Data obtained by these methods are presented and shown to be consistent at least within 1 per cent.

(over)

UNCLASSIFIED

1. Dielectric-Resonator Filters -- Analyses
1 Title Microwave Dielectric-Resonator Filters
II. Cohn, S. B and Kelly, K. C.
III Rantec Corp., Calabasas Calif
IV Contract DA 36-039-AMC-02267(E)

UNCLASSIFIED

AD DIV

The parameters affecting coupling between dielectric resonators are explained. Formulas are derived for the magnetic dipole moment and stored energy of the dielectric resonator. A generalized formula for coupling coefficient between two magnetic-dipole resonators is derived, and then particularized for the case of dielectric resonators spaced along the center-line of a cut-off rectangular waveguide.

Two pairs of dielectric resonators and three different sizes of waveguides were used to obtain six sets of coupling-coefficient data. The plotted curves can be utilized for design purposes. The measured values compare favorably to curves computed from the coupling-coefficient formula.

UNCLASSIFIED

UNITERMS

Filters
Dielectric-Constant
Resonator
Cylindrical
Rectangular
Isotropic
Magnetic-Dipole
Measurement
Microwave
Mode
Q
Coupling Coefficient
Stored Energy
TiO_2

UNCLASSIFIED

AD DIV

The parameters affecting coupling between dielectric resonators are explained. Formulas are derived for the magnetic dipole moment and stored energy of the dielectric resonator. A generalized formula for coupling coefficient between two magnetic-dipole resonators is derived, and then particularized for the case of dielectric resonators spaced along the center-line of a cut-off rectangular waveguide.

Two pairs of dielectric resonators and three different sizes of waveguides were used to obtain six sets of coupling-coefficient data. The plotted curves can be utilized for design purposes. The measured values compare favorably to curves computed from the coupling-coefficient formula.

UNCLASSIFIED

UNITERMS

Filters
Dielectric-Constnat
Resonator
Cylindrical
Rectangular
Isotropic
Magnetic-Dipole
Measurement
Microwave
Mode
Q
Coupling Coefficient
Stored Energy
TiO_2

UNCLASSIFIED

AD DIV

The parameters affecting coupling between dielectric resonators are explained. Formulas are derived for the magnetic dipole moment and stored energy of the dielectric resonator. A generalized formula for coupling coefficient between two magnetic-dipole resonators is derived, and then particularized for the case of dielectric resonators spaced along the center-line of a cut-off rectangular waveguide.

Two pairs of dielectric resonators and three different sizes of waveguides were used to obtain six sets of coupling-coefficient data. The plotted curves can be utilized for design purposes. The measured values compare favorably to curves computed from the coupling-coefficient formula.

UNCLASSIFIED

UNITERMS

Filters
Dielectric-Constant
Resonator
Cylindrical
Rectangular
Isotropic
Magnetic-Dipole
Measurement
Microwave
Mode
Q
Coupling Coefficient
Stored Energy
TiO_2

UNCLASSIFIED

AD DIV

The parameters affecting coupling between dielectric resonators are explained. Formulas are derived for the magnetic dipole moment and stored energy of the dielectric resonator. A generalized formula for coupling coefficient between two magnetic-dipole resonators is derived, and then particularized for the case of dielectric resonators spaced along the center-line of a cut-off rectangular waveguide.

Two pairs of dielectric resonators and three different sizes of waveguides were used to obtain six sets of coupling-coefficient data. The plotted curves can be utilized for design purposes. The measured values compare favorably to curves computed from the coupling-coefficient formula.

UNCLASSIFIED

UNITERMS

Filters
Dielectric-Constant
Resonator
Cylindrical
Rectangular
Isotropic
Magnetic-Dipole
Measurement
Microwave
Mode
Q
Coupling Coefficient
Stored Energy
TiO_2

UNCLASSIFIED

UNITED STATES ARMY ELECTRONICS RESEARCH & DEVELOPMENT LABORATORIES
STANDARD DISTRIBUTION LIST
RESEARCH AND DEVELOPMENT CONTRACT REPORTS

	Copies
OASD (R &E), Room 3E1065, ATTN. Technical Library, The Pentagon, Washington 25, D.C.	1
Chief of Research and Development, OCS, Department of the Army, Washington 25, D.C.	1
Commanding General, U.S. Army Materiel Command ATTN: R &D Directorate, Washington 25, D.C.	1
Commanding General, U.S. Army Electronics Command ATTN: AMSEL-AD, Fort Monmouth, New Jersey	3
Commander, Defense Documentation Center, ATTN: TISIA Cameron Station, Building 5, Alexandria, Virginia 22314	20
Commanding Officer, U.S. Army Combat Developments Command ATTN: CDCMR-E, Fort Belvoir, Virginia	1
Commanding Officer, U.S. Army Combat Developments Command Communications-Electronics Agency, Fort Huachuca, Arizona	1
Chief, U.S. Army Security Agency, Arlington Hall Station Arlington 12, Virginia	2
Deputy President, U.S. Army Security Agency Board Arlington Hall Station, Arlington 12, Virginia	1
Commanding Officer, Harry Diamond Laboratories, Connecticut Avenue and Van Ness Street, N.W., Washington 25, D.C.	1
Director, U.S. Naval Research Laboratory ATTN: Code 2027, Washington 25, D.C.	1
Commanding Officer and Director, U.S. Navy Electronic Laboratory San Diego 52, California	1
Aeronautical Systems Division, ATTN ASNXRR Wright-Patterson Air Force Base, Ohio 45433	1
Air Force Cambridge Research Laboratories, ATTN. CRZC L.G. Hanscom Field, Bedford, Massachusetts	1
Air Force Cambridge Research Laboratories, ATTN: CRXL-R L.G. Hanscom Field, Bedford, Massachusetts	1
Hq, Electronic Systems Division, ATTN. ESAT L.G. Hanscom Field, Bedford, Massachusetts	1
Rome Air Development Center, ATTN. RAALD Griffiss Air Force Base, New York	1
Advisory Group on Electron Devices, 346 Broadway, 8th Floor, New York, New York 10013	3
AFSC Scientific/Technical Liaison Office, U.S. Naval Air Development Center, Johnsville, Pennsylvania	1

ORIES

:S

	Copies
USAELRDL Liaison Office, Rome Air Development Center ATTN: RAOL, Griffiss Air Force Base, New York	1
NASA Representative (SAK/DL), Scientific and Technical Information Facility, P.O. Box 5700 Bethesda, Maryland 20014	2
Commander, U.S. Army Research Office (Durham) Box CM - Duke Station, Durham, North Carolina	1
Commanding Officer, U.S. Army Electronics Materiel Support Agency, ATTN: SELMS-ADJ, Fort Monmouth, New Jersey	1
Commanding Officer, Engineer Research and Development Laboratories, ATTN: Technical Documents Center Fort Belvoir, Virginia	1
Marine Corps Liaison Office, U.S. Army Electronics Research and Development Laboratories, Fort Monmouth, New Jersey	1
AFSC Scientific/Technical Liaison Office, U.S. Army Electronics Research and Development Laboratories, Fort Monmouth, New Jersey	1
Commanding Officer, U.S. Army Electronics Research and Development Laboratories, ATTN: Director of Research/ Engineering, Fort Monmouth, New Jersey	1
Commanding Officer, U.S. Army Electronics Research and Development Laboratories, ATTN: Technical Documents Center, Fort Monmouth, New Jersey	1
Commanding Officer, U.S. Army Electronics Research and Development Laboratories, ATTN: SELRA/ADO-RHA Fort Monmouth, New Jersey	1
	54

SUPPLEMENTAL DISTRIBUTION

Stanford Research Institute, ATTN: Dr. Matthaei Menlo Park, California	1
National Bureau of Standards, Engineering Electronics Section ATTN: Mr. Gustave Shapiro, Chief, Washington 25, D.C.	1
Chief, Bureau of Ships, Department of the Navy ATTN: Mr. Gumina, Code 68182, Washington 25, D.C.	1
Commander, Rome Air Development Center, ATTN: Mr. P. Romanelli (RCLRA-2), Griffiss Air Force Base, New York	1
Physical Electronic Laboratories, 1185 O'Brien Drive Menlo Park, California, ATTN: Dr. Carter	1
Commanding Officer, U.S.A. Electronics Research and Development Laboratories, Fort Monmouth, New Jersey	
ATTN: SELRA/PE (Division Director)	1
ATTN: SELRA/PE (Dr. E. Both)	1
ATTN. SELRA/PEM (Mr. N. Lipetz)	1
ATTN. SELRA/PEM (Mr. J. Charlton)	1
ATTN. SELRA/PEM (Mr. E. Mariani)	7